ELSEVIER

Thermochimica Acta 354 (2000) 71–80

thermochimica acta

www.elsevier.com/locate/tca

The nitridation kinetics of silicon powder compacts

Feg-Wen Chang*, Tzong-Horng Liou[1], Fu-Ming Tsai

Department of Chemical Engineering, National Central University, Chungli 32054, Taiwan

Received 22 November 1999; received in revised form 3 February 2000; accepted 5 February 2000

Abstract

The kinetics of the nitridation reaction of silicon powder compacts in a flowing 5% hydrogen/95% nitrogen stream over a temperature range of 1448–1648 K was investigated by thermogravimetry (TG). The effects of gaseous flow rate, pellet size, grain size, nitrogen concentration and reaction temperature on the nitridation reaction were extensively studied. The reaction order of the nitridation is found to be 0.71±0.03, and the activation energy of the reaction is 292±5 kJ mol^{-1}. A reaction mechanism, which includes the role of hydrogen in the nitridation system, is proposed to explain the experimental observations. The nitridation of a silicon pellet is mainly controlled by the diffusion of gaseous reactants through the product layer. A kinetic model of the nitridation process is developed which agrees well with the experimental results. © 2000 Elsevier Science B.V. All rights reserved.

Keywords: Silicon powder; Nitridation; Kinetics; Silicon nitride

1. Introduction

Important progress has been made in the development of engineering ceramic materials, especially the ceramics which are expected to be widely used in structural applications at high temperatures. Silicon nitride (Si_3N_4) is one of the most promising materials in this class. It has high hot-strength properties and hardness, good thermal-shock resistance and a low thermal- expansion coefficient. Moreover, the density of silicon nitride is only about one third of that of high-temperature superalloys. The foregoing properties make silicon nitride an excellent candidate for substituting strategic and critical metals such as tungsten, cobalt, chromium and nickel. The applications of silicon nitride are extensive, for example in machine tools, diesel engines, gas turbines, energy conversion system, heat exchangers, combustion chambers and material for ball and roller bearings.

High-quality powder is important in the fabrication of structural ceramics. The most prevalent method of silicon nitride preparation is the nitridation of silicon. It accounts for most of the silicon nitride produced because the process is simple and the original reactants Si and N_2 are abundant. This method consists of heating silicon in an atmosphere of nitrogen at elevated temperatures, ranging from 1373 to 1673 K. The basic chemical equation of the nitridation of silicon is as follows

$$3Si_{(s)} + 2N_{2(g)} \rightarrow Si_3N_{4(s)}, \quad \Delta H^0_{1623\,K} = -767\,kJ\,mol^{-1} \tag{1}$$

---

* Corresponding author. Tel.: +886-3-4227151, ext. 4202; fax: +886-3-4252296.

[1] Present address: Department of Chemical Engineering, Shu-Teh Junior College of Technology and Commerce, Taichung 402, Taiwan.

PII: S0040-6031(00)00432-9

Thermodynamic analysis indicates that the nitridation reaction is exothermic and favorable over the reaction temperature range involved. Various process variables, such as initial silicon particle size and purity, density and specific surface area, or the purity and pressure of reaction gas, have been the primary focus of the nitridation of silicon [1–6]. Most investigations of nitridation of silicon involve using silicon compacts. The gaseous flow rate ranges from 40 to 500 ml min^{-1}. The particle size of interest is below 100 μm. The extent of reaction progress is often determined by the gravimetric measurement. Messier and Wang [1] found that Fe impurities present in the compact accelerate the nitridation of silicon. Barsoum et al. [6] pointed out that, in the presence of hydrogen, the oxygen liberated reacts with the hydrogen and prevents the reoxidation of silicon, and thus enhances conversion. There have been several studies on the reaction between nitrogen and silicon to form silicon nitride; however, the kinetics of the nitridation of silicon compacts has not received much attention.

The present work investigates the effect of numerous process variables on the nitridation kinetics, including the gaseous flow rate, sample size, grain size of silicon powder, nitrogen gas concentration and reaction temperature. A thermogravimetric (TG) technique is used. We have also identified and characterized the physical properties of reactants and products. Moreover, all the results obtained provide information on the reaction rate, reaction mechanism and the kinetic model of nitridation.

2. Experimental

2.1. Materials used and sample preparation

The silicon powder (Johnson Matthey) used in these experiments had a purity of 99.999%. All powders used were screened through an ASTM standard sieve to obtain the desired grain-size range. This powder was pressed in a 1.3 cm diameter stainless steel die at 1.48×10^5 kPa to form a compact. The compact was then cut into spherical pellets with the desired diameters so as to minimize the touching distance between the sample and crucible. Finally, the spherical pellets were dried in a vacuum drier.

The sensitivity of the reaction between silicon and nitrogen to trace amounts of oxygen has been reported [6,7]. The oxygen inhibits the rate of nitridation by forming a thin protective film of silicon dioxide. It is better to add a small amount of hydrogen to the nitrogen to remove the thin film. Therefore, 5 vol.% H_2/95 vol.% N_2 was used as reaction gas with 5 vol.% H_2/95 vol.% Ar as purge gas in the experimental system. They were all made by San-Fu with a purity of 99.999%.

2.2. Experimental apparatus and procedure

Fig. 1 illustrates the experimental apparatus used for the nitridation measurements. The nitridation kinetic data were obtained using a thermogravimetric analyzer (Cahn, TG171) equipped with a sensitive recording electrobalance, an efficient furnace and a high-purity alumina tube. A computer was used for process control and data acquisition. The temperature was measured by a standard type-B thermocouple which was close to the molybdenum crucible. The crucible contained holes to prevent stagnant gas and to keep good contact between the pellet and the reaction gas. Before the reaction or purge gas was introduced into the reaction tube, they were passed through a deoxygenating column to further decrease the oxygen and water concentrations in the atmosphere. An experimental run was started by purging the system with 5 vol.% H_2/95 vol.% Ar before reaching the reaction temperature. The reaction gas of 5 vol.% H_2/95 vol.% N_2 then replaced the purge gas and was adjusted to the desired gaseous flow rate when the reaction temperature was reached.

2.3. Quantitative method

The overall reaction of the nitridation of silicon pellet is shown as Eq. (1) The degree of conversion of silicon, X_s, is defined as

$$X_s = \frac{W_s^0 - W_s}{W_s^0} \equiv \frac{-\Delta W_s}{W_s^0} \tag{2}$$

The initial weight of the pellet is equal to the initial weight of silicon. The weight gain of the pellet is equal to the consumption of nitrogen

$$W_p^0 = W_s^0 \tag{3}$$

$$\Delta W_p = -\Delta W_n \tag{4}$$

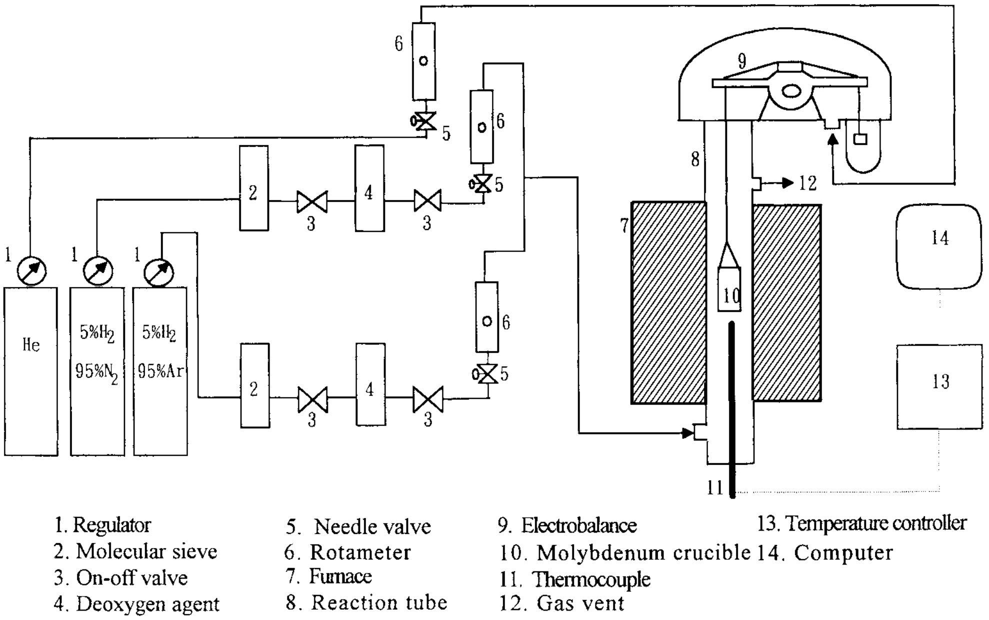

Fig. 1. Schematic diagram of the TG nitridation system.

From the stoichiometric coefficients of Eq. (1), the relationship between the consumption of silicon and nitrogen is

$$\frac{2(-\Delta W_s)}{M_s} = \frac{3(-\Delta W_n)}{M_n} \tag{5}$$

With a combination of Eqs. (2)–(5), the degree of conversion of silicon can be formulated as

$$X_s = \frac{3M_s \Delta W_p}{2M_n W_p^0} \tag{6}$$

According to Eq. (6), the conversion can be readily obtained from the initial silicon pellet weight (W_p^0) and the total weight change (ΔW_p) measured from TG.

2.4. Measurement of physical properties

The specific surface area of silicon powder was measured using a nitrogen adsorption method (Micrometric, ASAP 2000). The phase composition of the products was determined by X-ray diffraction (Siemens, D-500 diffractometer, Cu*K*α radiation). The microstructure and morphology of the reactants and products were studied using a scanning electron microscope (Hitachi, S-520).

3. Results and discussion

3.1. Analysis of physical properties

X-ray diffraction analysis reveals that the reacted silicon pellet contained unreacted silicon, α- and β-Si_3N_4. Silicon dioxide (SiO_2) and silicon oxynitride (Si_2N_2O) peaks are not observed. Moreover, the proportion of α-Si_3N_4 is much higher than that of β-Si_3N_4. Lindley et al. [7], Dervisbegovic and Riley [8], and Itoh [9] also found that the nitridation products have high α/β-Si_3N_4 ratios, when a hydrogen–nitrogen gas mixture was used as reaction gas.

The results of specific surface area analyses of the silicon powder under different grain sizes are given in Table 1. The specific surface area increases with decreasing silicon grain size. Pigeon and Varma [10] measured the specific area of silicon powder with grain sizes ranging from 5 to 37 μm and also found that finer powders have larger specific surface areas.

Scanning electron micrographs of the reactants and products are shown in Fig. 2. The silicon grains are nonporous and of a slightly irregular shape as shown in Fig. 2a. Figs. 2b–d illustrate the fracture surfaces of

Table 1
Effect of grain size on the specific surface area of silicon powder

Grain size (μm)	BET surface area ($m^2\,g^{-1}$)
<38	1.345
38–45	1.119
45–53	0.832
53–63	0.814
>63	0.383

pellets reacted at different reaction temperatures. Silicon nitride product layers have intimately covered the surface of the silicon. The results indicate that the N_2 gas molecules are chemisorbed onto the silicon surface, then the N_2 and Si react to form Si_3N_4. Product formed more deeply in the grain at 1623 K (Fig. 2c) than at 1448 K (Fig. 2d). However, the silicon grains were partially sintered when the reaction temperature was 1648 K as shown in the central part of Fig. 2b. Figs. 2e,f indicate that silicon nitride in whisker and needle forms is distributed within the vacant space between silicon grains. Similar morphology has also been observed by Jennings and Richman [11], and Jennings et al. [12]. The generally accepted explanation is that the needle form of silicon nitride is formed by a vapor–liquid–solid mechanism. The silicon vapor and N_2 react simultaneously at the solid–liquid interface to form needles of silicon nitride.

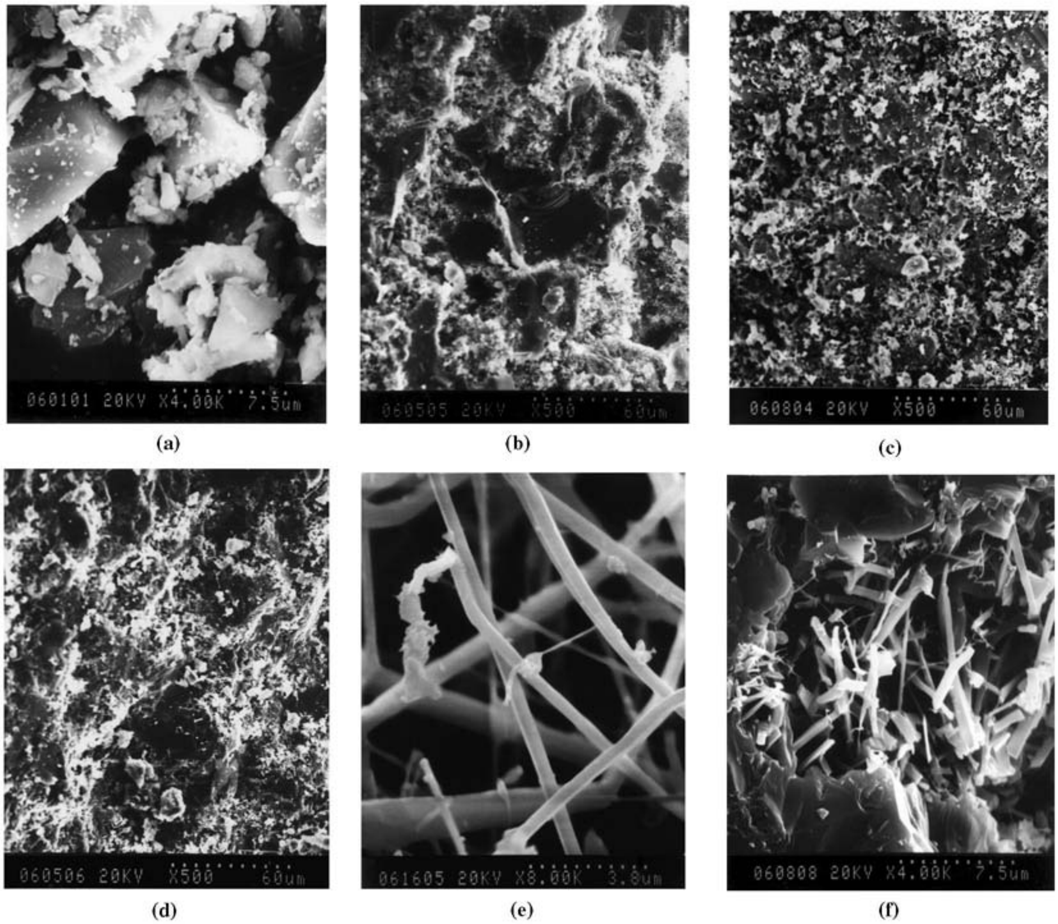

(a) (b) (c)

(d) (e) (f)

Fig. 2. Scanning electron micrographs of sample: (a) silicon powder (×4k); (b) nitridation pellet at 1648 K for 4 h (×500); (c) nitridation pellet at 1623 K for 4 h (×500); (d) nitridation pellet at 1448 K for 4 h (×500); (e) nitridation pellet at 1623 K (×8k); and (f) nitridation pellet at 1623 K (×4k).

3.2. Effect of gaseous flow rate

In order to obtain the intrinsic reaction rate between silicon grains and nitrogen, we must first exclude the resistance that arises from the external mass transfer of the pellet. The influence of gas film mass transfer can be decreased by increasing the gaseous flow rate.

Fig. 3 illustrates the nitridation reaction rate at different gaseous flow rates. The resistance due to gas film mass transfer does not affect the reaction rate when the gaseous flow rate increases from 50 to 600 ml min^{-1}. This indicates that the reaction gas concentration is uniform throughout the surface of the silicon pellet.

3.3. Effect of pellet size

When pore diffusion has a significant influence on the reactions between gases and pellets, concentration gradients of reaction gas exist within the pellet and the degree of conversion of the pellet is not uniform. Smaller pellet diameters provide shorter diffusion paths so as to decrease the resistance due to pore diffusion.

The effect of silicon pellet size on the nitridation reaction is shown in Fig. 4. When the pellet diameter is >9 mm, the reaction rate is obviously decreased, with pore diffusion playing a more important role. Therefore, the pellet diameter should be kept at <9 mm to ensure uniform concentration of reaction gas within the silicon pellet. The same conclusion has been reported by Liou and Chang [13,14] for the silicon dioxide/carbon mixture and pyrolyzed husk nitridation system.

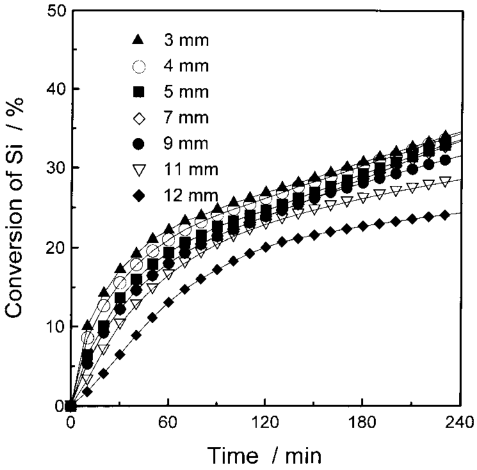

Fig. 4. The effect of pellet size on the nitridation of sample: gaseous flow rate, 400 ml/min; silicon grain size, <38 μm; reaction gas, 5% H_2/95% N_2; and reaction temperature, 1623 K.

3.4. Effect of silicon grain size

For the smaller silicon grain sizes, the nitridation rate is higher, as shown in Fig. 5. Finer powders also

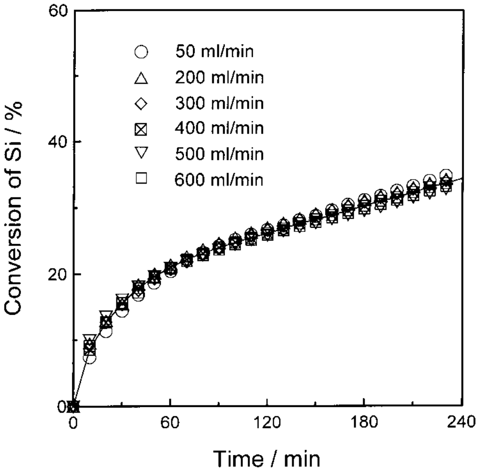

Fig. 3. The effect of gaseous flow rate on the nitridation of sample: pellet size, 4 mm; silicon grain size, <38 μm; reaction gas, 5% H_2/95% N_2; and reaction temperature, 1623 K.

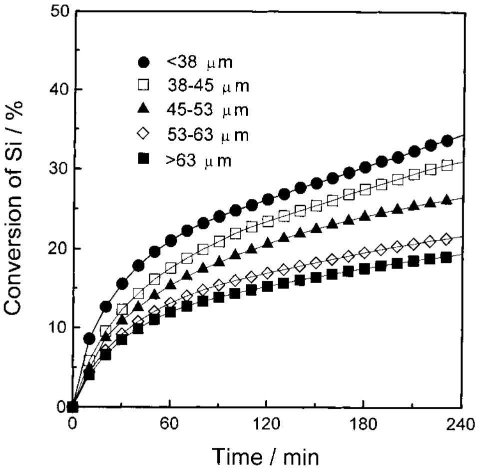

Fig. 5. The effect of silicon grain size on the nitridation of sample: gaseous flow rate, 400 ml/min; pellet size, 4 mm; reaction gas, 5% H_2/95% N_2; and reaction temperature, 1623 K.

have larger specific surface areas (Table 1). These results indicate that smaller grain sizes have larger reactive surface areas per unit mass and improve the contact between silicon and nitrogen, resulting in an increase in reaction rate. Pompe and Hermansson [15] used different silicon powders for their nitridation experiments, and found that the nitridation rate increased with increasing specific surface area. Silane-derived silicon powder was nitrided by Sheldon et al. [16], who discovered that high conversion could be reached even at a low temperature and within a short time if the powder is very fine and has a large specific area. Pigeon et al. [17] compared the nitridation of silicon powders of <43 µm and <250 µm, and found that the smaller size had the higher conversion. These observations agree with our present experimental results. Decreasing the silicon grain size increases not only the reactive surface area between silicon and nitrogen, but also the number of nucleation sites at which the Si_3N_4 can nucleate, and therefore enhances the conversion.

3.5. *Effect of nitrogen concentration*

The present investigation used 5 vol.% H_2/95 vol.% N_2 as reaction gas, and the mixed gas 5 vol.% H_2/95 vol.% Ar was used to regulate the concentration of the reaction gas. Therefore, the reaction gas always contained 5 vol.% H_2 in different concentrations of nitrogen so as to avoid the influence caused by the change in hydrogen concentration.

The conversion–time relationship of nitridation with different nitrogen concentrations is shown in Fig. 6. One can see that a lower nitrogen amount has reacted at a smaller conversion rate in a given time interval. The reason is obvious: argon is acting as an inert gas to dilute the nitrogen gas. This will decrease the probability of reaction between nitrogen and silicon, and slow down the rate of nitridation.

3.6. *Effect of reaction temperature*

The effect of reaction temperature on the conversion of silicon between 1448 and 1648 K is shown in Fig. 7. Faster reaction rates and greater overall conversions are observed with increasing reaction temperature. Atkinson et al. [18] carried out nitridation of silicon at temperatures between 1523 and 1633 K. Their results indicated that higher conversion was obtained with increasing temperature. Pigeon and Varma [10] studied the nitridation kinetics in the range from 1473 to 1623 K and also observed the same tendency.

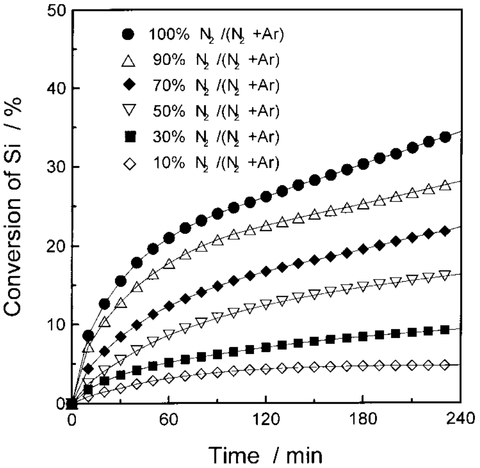

Fig. 6. The effect of nitrogen concentration on the nitridation of sample: gaseous flow rate, 400 ml/min; pellet size, 4 mm; silicon grain size, <38 µm; and reaction temperature, 1623 K.

In Fig. 7, almost all curves have the same characteristics. The initial part of the curve is approximately linear, and the latter part is approximately logarithmic. This illustrates that the formation of a silicon nitride layer during the reaction will gradually

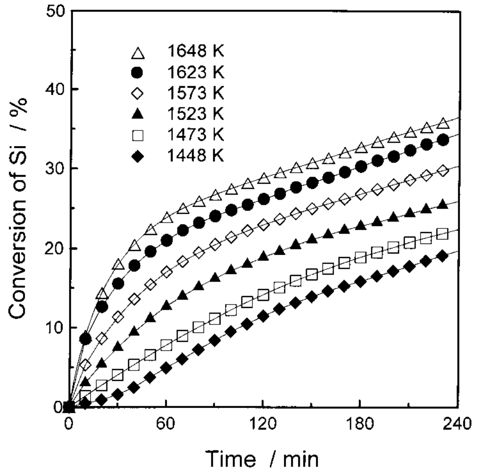

Fig. 7. The effect of reaction temperature on the nitridation of sample: gaseous flow rate, 400 ml/min; pellet size, 4 mm; silicon grain size, <38 µm; and reaction gas, 5% H_2/95% N_2.

cover the silicon surface, and decrease the reaction rate.

As the reaction between silicon and nitrogen is highly exothermic, increasing the reaction temperature will adversely affect the nitridation equilibrium. Reaction temperatures above 1683 K will result in the reactant (silicon) being melted or agglomerated, and decrease the reactive specific surface and, hence, the nitridation reaction rate.

A number of reported experimental results have suggested that the α-form of Si_3N_4 powder is more suitable for the fabrication of sinterable ceramic materials than the β-form. α-Si_3N_4 is formed at temperatures (<1773 K) lower than those required for the formation of the β-Si_3N_4. Therefore, in order to obtain silicon nitride powder of high quality, the reaction temperature must be optimized and nitridation should be performed below the melting point (<1683 K) of silicon.

3.7. Intrinsic reaction rate expression

When resistance due to mass transfer is excluded and the silicon grain size does not affect the reaction rate, the rate equation for nitridation of silicon can be represented as:

$$-r_s = f(k, y_n) \equiv k y_n^n \tag{7}$$

Taking natural logarithms, we obtain

$$\ln(-r_s) = \ln k + n \ln(y_n) \tag{8}$$

The order with respect to the nitrogen concentration can be determined by Eq. (8). A plot of $\ln(-r_s^0)$ vs. $\ln(y_n)$ is shown in Fig. 8. From the plot, an order of 0.71±0.03 for the nitrogen concentration is obtained.

Using the Arrhenius equation, Eq. (7) can be written as

$$k = \frac{-r_s^0}{(y_n)^n} \equiv k_0 \exp\left(\frac{-E_a}{RT}\right) \tag{9}$$

Taking natural logarithms yields

$$\ln k = \ln\left(\frac{-r_s^0}{y_n^n}\right) \equiv \ln k_0 - \frac{E_a}{RT} \tag{10}$$

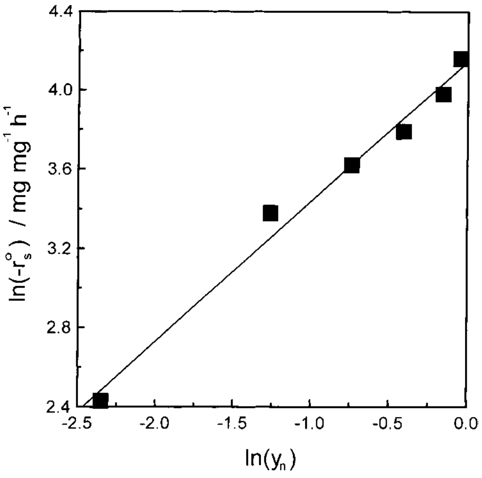

Fig. 8. The effect of nitrogen concentration on the initial nitridation rate of silicon: gaseous flow rate, 400 ml/min; pellet size, 4 mm; silicon grain size, <38 μm; and reaction temperature, 1623 K.

An Arrhenius plot is shown in Fig. 9. The activation energy of the silicon pellet nitridation reaction is 292±5 kJ mol^{-1}. The rate expression for the nitridation of a silicon pellet can be represented by the equation:

$$-r_s = 1.70 \times 10^{11} \exp\left(\frac{292 \times 10^3}{RT}\right) y_n^{0.71} \quad (\mathrm{mg\ mg^{-1}\ h^{-1}}) \tag{11}$$

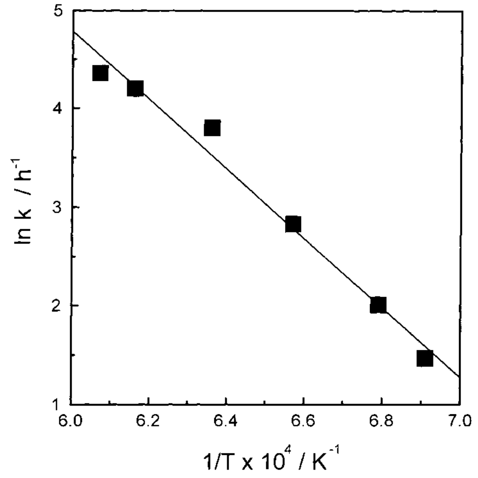

Fig. 9. Arrhenius plot showing the temperature dependence of the initial nitridation rate of silicon: gaseous flow rate, 400 ml/min; pellet size, 4 mm; silicon grain size, <38 μm; and reaction gas, 5% H_2/95% N_2.

The activation energy reported in this work is similar to that observed by Pigeon and Varma [10] of 301.5 kJ mol^{-1}. It is also found that the activation energy of the nitridation of silicon pellet is distinctly lower than that of pure silicon dioxide/carbon mixture which is 448 kJ mol^{-1} (Liou and Chang [13]). In a pure silicon dioxide/carbon mixture system, the chemical bonding between silicon and oxygen is extremely intimate, and hence, a higher energy must be provided to dissolve the silicon dioxide so as to continue the nitridation reaction.

3.8. Formulation of a reaction mechanism

The formation of silicon nitride from silicon probably occurs by several paths. According to the experimental observations, a simplified mechanism for the silicon compact and nitrogen/hydrogen system can be constructed.

The main reactants in the system are silicon, nitrogen and hydrogen. As mentioned earlier, the role of hydrogen is to remove the oxide film and to accelerate the nitridation rate. The removal of the film by the intermediate SiO will encourage the formation of α-Si_3N_4 [7–9]. Jennings et al. [12,19] suggested that the formation of α-Si_3N_4 resulted from silicon complexing with molecular nitrogen, while that of β-Si_3N_4 resulted from atomic nitrogen. In our experiments, X-ray diffraction analysis reveals that the main product is α-Si_3N_4. This result indicated that molecular nitrogen is a major gaseous component during the nitridation reaction.

From SEM observations, it is clear that the silicon nitride product layer has intimately covered the surface of the silicon. This result indicated that, at the beginning of nitridation reaction, nitrogen molecules must be adsorbed on the silicon surface before reacting, then silicon monoxide (or silicon) reacts with the molecular nitrogen to form α-Si_3N_4 nuclei on the silicon surface (nucleation reaction). After nuclei are formed, more silicon and nitrogen will continue to be transported to the reaction site to form the Si_3N_4 thin layer (growth reaction). As the thickness of the layer gradually increases, the nitridation rate is decreased and the reaction is mainly controlled by the diffusion of the gaseous reactants through the product layer.

In addition, the SEM observations also show whisker and needle forms of Si_3N_4 distributed within the vacant space between silicon grains. This means that only a fraction of the nitridation reaction occurs within a pellet, with most Si_3N_4 being formed in the void between grains. This result indicates that the silicon (or silicon vapor) may be transported out of the void through the product layer. Simultaneously, nitrogen molecules diffuse through the microscopic vacant space and combine with silicon to form Si_3N_4.

According to the foregoing observations, the nitridation mechanism occurs in two main stages. In the first stage, the outer surface of the silicon particle is predominantly a silica film. In the presence of hydrogen, the film is converted to silicon monoxide and then the nitridation reaction continues to proceed. The reactions occurring in this stage are:

$$\mathrm{SiO}_{2(s)} + \mathrm{H}_{2(g)} \rightarrow \mathrm{SiO}_{(g)} + \mathrm{H_2O}_{(g)},\quad G^0_{1623\,\mathrm{K}} = 229\ \mathrm{kJ\,mol^{-1}} \tag{12}$$

$$3\mathrm{SiO}_{(g)} + 2\mathrm{N}_{2(g)} \rightarrow \mathrm{Si_3N}_{4(s)} + \tfrac{3}{2}\mathrm{O}_{2(g)},\quad \Delta G^0_{1623\,\mathrm{K}} = 502\ \mathrm{kJ\,mol^{-1}} \tag{13}$$

After the protective silica film is removed, the inner zone of the compact is pure silicon, and the second stage of the nitridation reaction then proceeds in accordance with Eq. (1), for which $\Delta G^0_{1623\,\mathrm{K}} = -208$ kJ mol^{-1}. Thermodynamic calculations [20] indicate that reactions (12) and (13) have positive Gibbs energies over the reaction temperature range. The occurrence of reaction indicates that the interaction between silicon and oxygen is much stronger, and therefore a higher energy is needed to continue the nitridation reaction. However, Eq. (1) is thermodynamically favored, so that removal of the protective silica film in the initial nitridation stage is important to enhance the entire reaction rate effectively.

The proposed mechanism can be summarized as follows:

(a) The presence of hydrogen in the nitriding gas is to remove the protective silica film on the silicon surface and to enhance the nitridation rate.

(b) Nitrogen molecules are chemisorbed onto the silicon surface. Nuclei of silicon nitride are formed on the silicon surface in the initial stage of the nitridation.

(c) The reactants (silicon or nitrogen) diffuse on the surface of the nuclei to continue the nitridation reaction. The silicon nitride product layer is gradually formed.

(d) When the Si_3N_4 layer has thickened to cover the silicon surface completely, the reaction rate will gradually decrease, and the reaction is mainly controlled by the diffusion of the gaseous reactants through the product layer.

4. Kinetic model

In the nitridation reaction system, the presence of O_2 or H_2 in the system will increase the complexity of the kinetics and the process will not be governed by a simple rate-controlling step. Various models have been proposed to explain the nitriding kinetics data. In order to establish the possible functions of hydrogen within a nitriding compact, Dervisbegovic and Riley [7] proposed a two-zone model for the reaction of silicon powder compact in normal nitrogen/hydrogen atmosphere; while Pigeon and Varma [10] suggested a sharp-interface model (SIM) with product layer expansion under conditions of diffusion control.

In our model of the nitridation reaction, the silicon pellet is assumed to consist of a number of small spherical grains [21]. The grains are ordinarily nonporous and, within each grain, the reaction front retains its original spherical shape. When the pellet reacts in the absence of external mass transport resistance and is controlled by diffusion through the product layer around the grains, the rate of diffusion through the product layer is given by:

$$-4\pi r^2 D_e \frac{dC_n}{dr} = C_1 \tag{14}$$

where C_n is concentration of nitrogen, D_e the effective diffusivity of nitrogen through product layer, and r the grain radius of silicon.

The boundary conditions are

$$C_n = 0 \quad \text{at } r = r_c \tag{15}$$

and

$$C_n = C_n^0 \quad \text{at } r = r_0 \tag{16}$$

Integrating Eq. (14), the constant C_1 can be evaluated from the boundary conditions. Then, the rate of reaction of the silicon grain can be obtained by

$$\frac{3}{2}4\pi r^2 D_e \frac{dC_n}{dr} = \frac{3}{2}\frac{4\pi D_e C_n^0}{(1/r_c - 1/r_0)} \equiv \frac{6\pi D_e C_n^0}{(1/r_c - 1/r_0)} \tag{17}$$

The reaction rate of a silicon grain can also be represented by

$$4\pi r^2(-r_{sg}) = -\frac{dN_{sg}}{dr} \equiv \frac{6\pi D_e C_n^0}{(1/r_c - 1/r_0)} \tag{18}$$

where

$$N_{sg} = \frac{W_s}{NM_s} \tag{19}$$

$$W_s = \tfrac{4}{3}\rho_s \pi N r_c^3 \tag{20}$$

Combining Eqs. (18)–(20) and rearranging, we can obtain the overall reaction rate of silicon as follows

$$-\frac{1}{W_s^0}\frac{dW_s}{dt} = \frac{6\pi C_n^0 D_e N M_s}{(4/3\rho_s \pi N)^{1/3} W_s^0 [W_s^{-1/3} - (W_s^0)^{-1/3}]} \tag{21}$$

Integrating Eq. (21) and using the definition of conversion (Eq. (2)), the relationship between conversion and reaction time can be expressed [21] as

$$1 - 3(1 - X)^{2/3} + 2(1 - X) = k_1 t \tag{22}$$

where

$$k_1 = \frac{12\pi C_n^0 D_e N M_s}{(4/3\rho_s \pi N)^{1/3} (W_s^0)^{2/3}} \tag{23}$$

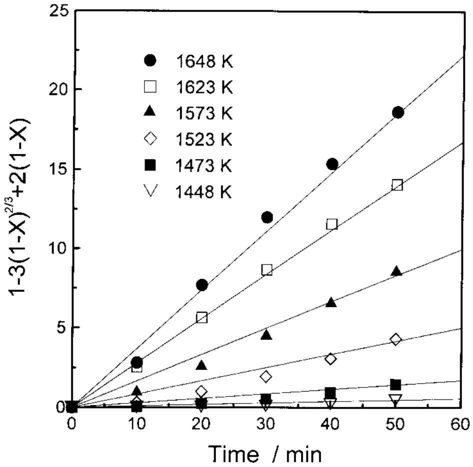

Fig. 10. Conversion–time data at different constant temperatures: gaseous flow rate, 400 ml/min; pellet size, 4 mm; silicon grain size, <38 µm; and reaction gas, 5% H_2/95% N_2.

The experimental conversion–time data at different constant temperatures are shown in Fig. 10. It can be seen that the relationship is linear and indicates that the diffusion of N_2 through the product layer of the grain is the rate-controlling step.

Nomenclature

C_n	concentration of nitrogen (mol mm^{-3})
D_e	effective diffusivity of nitrogen through Si_3N_4 product layer (mm^2 h^{-1})
E_a	activation energy (kJ mol^{-1})
k	initial rate constant (h^{-1})
k_0	pre-exponential factor (h^{-1})
k_1	rate constant in Eq. (22) (h^{-1})
M_i	molecular weight of component i
N	number of silicon grains in pellet
N_{sg}	mol of silicon in each grain
n	reaction order of nitrogen
R	gas constant=8.314 (J mol^{-1} K^{-1})
r	grain radius of silicon (mm)
r_c	radius of unreacted core of silicon grain (mm)
r_0	initial grain radius of silicon (mm)
$-r_s$	reaction rate of silicon (mg mg^{-1} h^{-1})
$-r_{sg}$	reaction rate of silicon grain (mol mm^{-2} h^{-1})
T	reaction temperature (K)
t	reaction time
W_n	weight of nitrogen (mg)
W_p	total weight of pellet at time t (mg)
W_s	weight of silicon in pellet (mg)
X_s	conversion of silicon
y_n	volume fraction of nitrogen

Superscript

0	initial condition

Subscripts

n	nitrogen
p	pellet
s	silicon

Greek symbols

ρ_s	density of silicon in the pellet (kg m^{-3})
Δ	change in property

Acknowledgements

The authors would like to thank the National Science Council of Taiwan for its financial support under Project NSC 84-2214-E008-002.

References

[1] D.R. Messier, P. Wong, J. Am. Ceram. Soc. 56 (1973) 480.
[2] D. Campos-Loriz, F.L. Riley, J. Mater. Sci. 11 (1976) 195.
[3] D.P. Elias, M.W. Lindley, J. Mater. Sci. 11 (1976) 1278.
[4] M.N. Rahaman, A.J. Moulson, J. Mater. Sci. 19 (1984) 189.
[5] B.W. Sheldon, J.S. Haggerty, Ceram. Eng. Sci. Proc. 10 (1989) 784.
[6] M. Barsoum, P. Kangutkar, M.J. . Koczak, J. Am. Ceram. Soc. 74 (1991) 1248.
[7] H. Dervisbegovic, F.L. Riley, J. Mater. Sci. Lett. 14 (1979) 1265.
[8] M.W. Lindley, D.P. Elias, B.F. Jones, K.C. Pitman, J. Mater. Sci. 14 (1979) 70.
[9] T. Itoh, J. Mater. Sci. Lett. 9 (1990) 19.
[10] R.G. Pigeon, A. Varma, Chem. Eng. Sci. 47 (1992) 2585.
[11] H.M. Jennings, M. Richman, J. Mater. Sci. 10 (1975) 967.
[12] H.M. Jennings, B.J. Dalgleish, P.L. Pratt, J. Mater. Sci. 23 (1988) 2573.
[13] T.H. Liou, F.W. Chang, Ind. Eng. Chem. Res. 34 (1995) 118.
[14] T.H. Liou, F.W. Chang, Ind. Eng. Chem. Res. 35 (1996) 3375.
[15] R. Pompe, L. Hermansson, Mater. Sci. Eng. 71 (1985) 355.
[16] B.W. Sheldon, J. Szekely, J.S. Haggerty, J. Am. Ceram. Soc. 75 (1992) 677.
[17] R.G. Pigeon, A. Varma, A.E. Miller, J. Mater. Sci. 28 (1993) 1919.
[18] A. Atkinson, A.J. Moulson, E.W. Roberts, J. Am. Ceram. Soc. 59 (1976) 258.
[19] H.M. Jennings, J. Mater. Sci. 18 (1983) 951.
[20] M.W. Chase Jr., C.A. Davies, J.R. Downey, D.J. Frurip, R.A. Mcdonald, A.N. Syverud, J. Phys. Chem. Ref. Data 14 (1985) 1260.
[21] J. Szekely, J.W. Evans, H.Y. Sohn, Gas–Solid Reaction, Academic Press, New York, 1976, p. 75.